ELSEVIER

Journal of Molecular Catalysis A: Chemical 176 (2001) 205–212

JOURNAL OF MOLECULAR CATALYSIS A: CHEMICAL

www.elsevier.com/locate/molcata

Effect of hydrogenation under high pressure on the structure and catalytic properties of Cu–Zr amorphous alloys

A. Szummer [a], M. Janik-Czachor [b], Á. Molnár [c,*], I. Marchuk [b], M. Varga [c], S.M. Filipek [b]

[a] *Faculty of Material Science, Technical University, Warsaw, Poland*
[b] *Institute of Physical Chemistry, Polish Academy of Sciences, Kaprzaka 44/52, 01-224 Warsaw, Poland*
[c] *Department of Organic Chemistry, University of Szeged, Dóm tér 8, H-6720 Szeged, Hungary*

Received 3 January 2001; accepted 8 June 2001

Abstract

Hydrogenation under high pressures up to 3 GPa and at elevated temperatures up to 393 K was used to introduce structural changes in the bulk and on the surface of Cu–Zr amorphous alloys which then were examined by XRD and microscopy. The hydrogenative pre-treatment at a high hydrogen fugacity followed by annealing at 623 K, aimed at desorption of hydrogen, and an eventual exposure of the samples to air at room temperature to oxidize Zr, resulted in a distinct increase of catalytic activity in the dehydrogenation of 2-propanol. A tentative mechanism to account for enhancing the catalytic activity induced by the above combined pre-treatment including correlations between catalytic performance (activity, selectivity) and physical characteristics (morphology, XRD features, Cu(0) specific surface areas) is discussed.

Keywords: Amorphous alloys; Hydrogen treatment; Dehydrogenation; 2-Propanol; Activity enhancement

1. Introduction

Zirconium-containing amorphous alloys (AA) have attracted quite significant attention in recent years as precursors of efficient and durable catalysts for a number of technically important chemical reactions [1–6]. Various procedures of activation aimed at transforming the original amorphous ribbons of low surface area into efficient and stable catalysts have been developed. Among these, the most effective techniques are aging in air, etching, i.e. partial dissolution of Zr with dilute HF solution [7–10], and in situ activation occurring during alcohol dehydrogenation over Cu–Zr [8], ammonia synthesis over Fe–Zr [11] or exposing Zr-containing alloys (Cu–Zr, Au–Zr, Ni–Zr, Pd–Zr) to CO_2 hydrogenation [12–14] or CO oxidation conditions [15,16]. As our own experiences with Cu–Zr amorphous alloy ribbons have shown, electrochemical modification is also an efficient pre-treatment which significantly increases catalytic activities in the dehydrogenation of alcohols [17–19].

In contrast, the effect of gaseous hydrogen at atmospheric pressure on the catalytic activity is found to be moderate even after prolonged application at elevated temperature [8,20–22]. Studies using such hydrogenative pre-treatment [22–25] or charging the sample electrochemically with hydrogen [26,27] have indicated significant changes in both the bulk and the surface structure. One can anticipate that the possible changes in the catalytic activity of such pre-treated

* Corresponding author. Tel.: +36-62-544-277; fax: +36-62-544-200.
E-mail address: amolnar@chem.u-szeged.hu (Á. Molnár).

1381-1169/01/$ – see front matter
PII: S1381-1169(01)00259-X

materials could be correlated with the newly developed structure containing small copper particles embedded in the amorphous matrix. It is quite surprising, therefore, that the effect of high pressure hydrogenation of zirconium-containing amorphous ribbons on their catalytic performance has not been investigated. Hydrogen treatment at high pressure is known to bring about significant structural changes in the bulk and on the surface [28–30]. These changes result from the dissolution of a large amount of hydrogen in the amorphous matrix or, eventually, segregation of its components, depending upon temperature. The changes brought about by hydrogenation of Cu–Zr alloys are as follows: (i) the samples become brittle; (ii) the specific surface area increases; (iii) the inter-atomic distances increase; (iv) Cu segregation is enhanced because of the formation of Zr hydride. Moreover, the high pressure hydrogen treatment of Cu–Zr AA markedly reduces the temperature of crystallization. Naturally, the crystallization products differ significantly when the crystallization process is carried out during high pressure hydrogenation or in an inert gas atmosphere. Such a pre-treatment, therefore, may be of interest as a useful process to induce the necessary transformations leading to the development of catalytically active materials.

In conclusion, an analysis of the relevant literature data show that (i) hydrogen treatment of amorphous Cu–Zr samples at atmospheric pressure induces important structural changes; (ii) samples, thus, prepared may exhibit improved catalytic properties; (iii) structural changes brought about by hydrogen treatment at high pressure are even more significant. It follows that hydrogenation of Cu–Zr at high pressure may be expected to result in catalytic materials with even better catalytic performance. The aim of this work, therefore, is to examine the effects of a high pressure hydrogenative treatment of Cu–Zr amorphous ribbons on their structure and catalytic properties.

2. Experimental

2.1. Materials and microscopic examinations

Cu–Zr AA ribbons (60Cu–40Zr or 50Cu–50Zr) produced by melt spinning method were 4 mm wide and ∼40 μm thick. Two kinds of the ribbons were used for the investigations: freshly cast, or aged in air for 8 months up to 12 years, with a visible partial devitrification. 2-Propanol was purchased from Aldrich.

X-ray diffraction (XRD) analysis was carried out by a Rigaku diffractometer using Cu Kα radiation. The samples were examined with an optical microscope, and an electron microprobe Cameca Semprobe SU30 instrument equipped with wavelength/energy dispersive spectrometry (WDS/EDS) and scanning electron microscopy (SEM) facilities. This equipment enabled us to monitor surface morphology and composition.

The following surface corrosion/devitrification products were analyzed:

1. the surface oxide zone on both sides of the ribbon;
2. the red islands formed at the wheel side of the ribbons;
3. carefully polished cross-sections of the surface zone of the ribbon. To obtain such a cross-section a piece of the ribbon was mounted into epoxy to protect the peculiar structure of the wheel side, and then carefully polished to reveal the structure of the cross-section.

The specimens after the microscopic examinations were subjected to hydrogenation under high pressure and subsequently to a catalytic test as described below.

2.2. Hydrogenation under high pressure

A high pressure piston–cylinder apparatus described elsewhere [28,31] was used for hydrogen or deuterium compression up to about 3 GPa. The temperature of the apparatus was controlled up to 393 K; for higher temperatures samples were heated in a special small electric furnace placed in the pressure vessel. H/Cu–Zr ratios were determined by elemental analysis or by mass spectrometry.

2.3. Heat treatment/air exposure

Some of the hydrogenated samples were additionally heat treated in helium at 623 K to desorb hydrogen. The resulting material was then exposed to air at room temperature for controlled time intervals in order to allow Zr to oxidize.

2.4. Catalytic test

Dehydrogenation of 2-propanol was chosen to test the changes in the catalytic activity of the Cu–Zr ribbons. About 15 mg of either the as-received, aged or the pre-treated ribbon samples was loaded into a glass microreactor. 2-Propanol was fed by a microfeeder into a stainless steel evaporator, where it was mixed with hydrogen (used in order to activate Cu–Zr ribbons). Then the gas mixture (2-propanol/hydrogen molar ratio = 0.018) was introduced into the reactor kept at 573 K. The total flow rate was 10 ml min^{-1}. The reactor temperature was controlled to an accuracy of 0.5 K by using a microprocessor based controller (Selftune plus, LOVE Controls). The effluents sampled by a pneumatic gas sampling system were analyzed by GC (Shimadzu 8A equipment, thermal conductivity detector, CWAX 20M column, 343 K, 25 ml min^{-1} flow rate of helium carrier gas). The gases used were of high purity (hydrogen = 99.9990%, helium = 99.996%). Calculations were made by applying a Data Apex Chromatography Station for Windows 1.5.

The Cu(0) surface area of the samples was measured by N_2O titration at 363 K based on the reaction of nitrous oxide with Cu(0) species using the GC pulse method. A short hydrogen treatment (30 min at 563 K) was applied before measurements.

3. Results and discussion

Examinations of the as-received ribbons confirm the previous investigations [19,30,32], specifically, the freshly fabricated Cu–Zr amorphous alloys are covered by a thin (0.6–0.8 nm) ZrO_2 layer which is not visible at the magnification applied, but it is well detectable with AES [32]. This layer is defective at the wheel side. When the ribbon is kept in air (aged) oxidation proceeds there with a concomitant Cu segregation. This devitrification process results in the development of a "sandwich structure" of crystalline Cu/ZrO_2 bilayer or multilayer [19,32]. The thickness of such a devitrified zone is about 2–3 μm, thus, not exceeding 10% of the original thickness of the ribbon [32]. The bulk of the ribbon, however, remains amorphous, hence highly homogeneous, with no visible microscopic contrast. The surface features of such a Cu–Zr sample aged in air for 12 years are presented in Fig. 1.

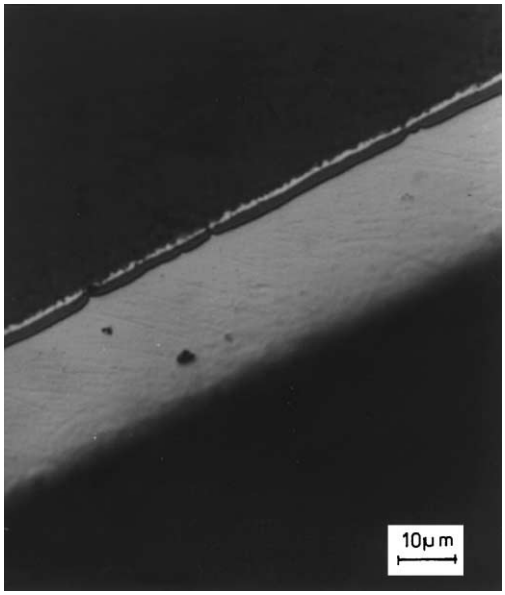

Fig. 1. A typical optical micrograph of a cross-section of a Cu–Zr ribbon aged in air for 12 years. The thickness of the devitrified zone (rough surface Cu layer plus violet, seen here as black, smooth ZrO_x under-layer) does not exceed ~10% of the total thickness of the ribbon. The inside of the ribbon remains homogeneous (amorphous) without any visible microscopic contrast.

As indicated in Section 2, samples were treated with either hydrogen or deuterium with the aim of exploring possible isotope effects. However, no distinct isotope effect was observed with respect to morphology, structure (as determined by XRD), and Cu segregation phenomena. Consequently, only the results of hydrogenative pre-treatment will be discussed.

The hydrogen treatment at 302 K of ribbons with this devitrified zone on top resulted in an extremely slow absorption kinetics even at pressures as high as 2.7 GPa. For example, after 100 h of exposure the H/Cu–Zr ratio for 50Cu–50Zr was as low as 0.07. It was found, however, that after the mechanical removal of the thin (2–3 μm) devitrified surface layer, the hydrogen absorption process accelerated considerably [30]. An increase in temperature resulted in the same effect. All further investigations, therefore, were performed at elevated temperatures with samples without the surface devitrified zone to enhance the entry of hydrogen into the bulk of the AA.

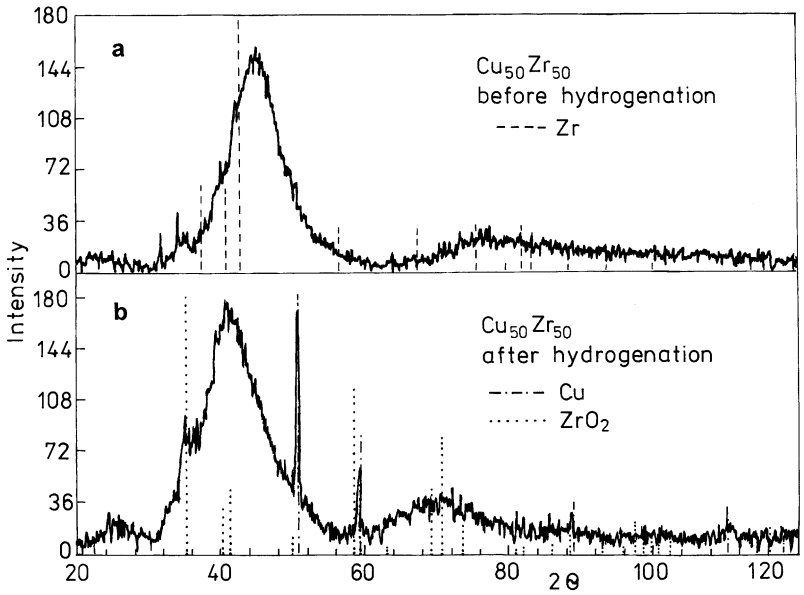

Fig. 2. XRD pattern for 50Cu–50Zr amorphous alloy: (a) before hydrogenation; (b) after hydrogenation at 373 K, 1 GPa for 3 days.

For 50Cu–50Zr alloy a 75 h exposure to 1.1 GPa hydrogen at 373 K resulted in the attainment of an atomic ratio of H/Cu–Zr = 1.2, whereas at 302 K this ratio was only about 0.3. The samples undergoing hydrogen treatment became brittle. The high brittleness of these samples provided an easy way to obtain a material with a high specific surface area, since they disintegrate into small pieces at a simple touch. However, new surface areas open up for further oxidation of Zr resulting in devitrification with concomitant Cu segregation.

Fig. 2(a) shows the typical XRD pattern of a 50Cu–50Zr amorphous ribbon, with no devitrified surface layer on top. Only a broad maximum, characteristic of an amorphous phase is visible. Fig. 2(b) represents the XRD pattern after hydrogenation under a high pressure (373 K, p_{H_2} = 1 GPa, 3 days). Hydrogen charging has shifted the broad amorphous peak to lower angles, thus, indicating an increase in the inter-atomic distances within the alloy due to hydrogen absorption. Moreover, distinct diffraction lines from crystalline Cu appear, suggesting a partial crystallization of copper. Similar changes were observed for the other alloy with a different Cu content.

Fig. 3 shows micrographs of a hydrogenated sample (393 K, p_{H_2} = 0.12 GPa, 70 h) which was additionally annealed for 30 min at 623 K to desorb hydrogen. Apparently, absorption and desorption of hydrogen resulted in a partial devitrification on both sides of the ribbon. Distinct particles (red) of Cu are visible. On the free side, they are smaller by a factor of 2–3 than those on the wheel side (compare Fig. 3(a) and (b)).

Fig. 4 represents the results of the catalytic tests (activities in the dehydrogenation of 2-propanol) for a 60Cu–40Zr amorphous ribbon. In Fig. 4(A) catalytic properties of the samples without hydrogenative pre-treatment are collected. It is seen that the activity of the catalyst after oxidative treatment is practically identical with that of the as-received alloy. The third set of data refers to the catalyst sample with the thin devitrified surface layer mechanically removed. This sample exhibits almost negligible activity. These data indicate that the oxidized surface layer plays a crucial role in activity, but a simple oxidation is not an effective method to increase catalytic efficiency.

Fig. 4(B) gives the results of catalytic tests for the hydrogen-treated samples. Catalytic efficiency of the hydrogenated ribbon is distinctly lower than that without any preceding hydrogenation (compare Fig. 4(A) plot a with Fig. 4(B) plot a). Thus, the rather homogeneous Zr–Cu–H ternary amorphous alloy with the expanded inter-atomic distances between the metal

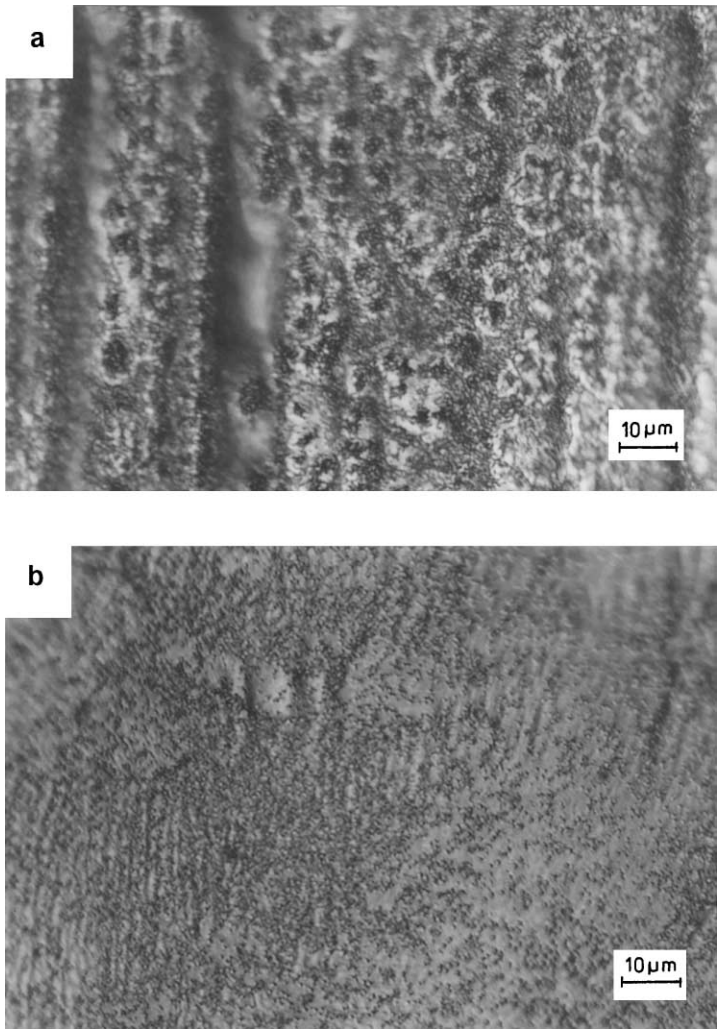

Fig. 3. Morphology of a 40Cu–60Zr glassy ribbon after hydrogenation at 393 K, $p_{H_2} = 0.12$ GPa, 70 h, then annealed for 30 min at 623 K to desorb hydrogen. Visible particles of crystalline Cu (red) are clearly distinguishable at the surface: (a) wheel side; (b) free side.

atoms and the embedded therein small clusters of partly crystallized Cu is not an efficient catalyst for the test reaction.

The specific surface areas of the two catalyst samples show some interesting changes. The as-received alloy does not have any measurable Cu(0) surface. In contrast, the used sample does exhibit a Cu(0) surface area of $0.17\,m^2\,g^{-1}$. The development of a stable working catalyst from an amorphous precursor under reaction conditions with the concomitant increase in specific surface is a well-known phenomenon [2]. The interaction of reactant molecules with the surface, and the effect of hydrogen and oxygen impurities present are suggested to account for the observed changes. This phenomenon is even more pronounced for the hydrogen-treated sample: the catalyst after reaction has a Cu(0) surface area of $0.50\,m^2\,g^{-1}$. What is surprising, however, is that this catalyst is inferior to the untreated, but aged sample despite the larger specific surface area.

A probable explanation is the following. Dehydrogenation of alcohols is known to require active sites

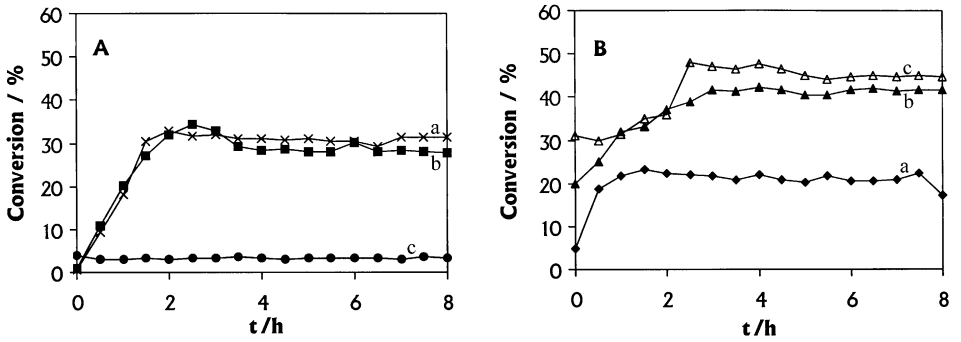

Fig. 4. Efficiency for the conversion of 2-propanol as a function of reaction time over a 1-year old amorphous 60Cu–40Zr alloy. (A) Before any pre-treatment, plot a (×); after oxidative pre-treatment (473 K, 3 h), plot b (■); after the mechanical removal of the devitrified Cu/ZrO_x surface layer, plot c (●). (B) The ribbon additionally modified by hydrogenation (393 K, $p_{H_2} = 0.12$ GPa, 70 h), plot a (◆); pre-treated as in plot a followed by annealing at 623 K for 5 h in flowing helium and additionally exposed to air for 2 days, plot b (▲); pre-treated as in plot b, but with longer air exposure (9 days), plot c (△).

composed of two surface entities. The reacting alcohol chemisorbs on a metallic site (Cu atom) resulting in the formation of a surface alkoxide group, but the adsorption of hydrogen formed requires the participation a surface oxygen. The cleavage of the C–H bond to yield the product carbonyl compound, again, takes place with the interaction of copper. This interpretation is supported by surface science studies [33,34] and by data showing synergism between copper and its oxides in dehydrogenation [35]. We may suggest that the large amount of hydrogen charged into the AA and released during reaction serves as an oxygen scavenger thereby preventing the formation of surface oxide sites necessary for alcohol chemisorption to start the dehydrogenation process.

However, after further pre-treatment, specifically, after desorption of the hydrogen at 623 K and subsequent exposure to air, the catalytic efficiency of the material gradually increases (compare plot a with plots b and c in Fig. 4(B). As seen the catalytic efficiency of the hydrogenated ribbon is higher than that with the thin surface oxide layer removed, but is distinctly lower than the activities after air exposure). These results point to the beneficial role of oxidation of Zr in the overall catalytic process. One may suggest that at least a partial oxidation of a large, freshly developed surface of a rather brittle Cu–Zr material leads to the segregation and, eventually, precipitation of copper to the surface and a suitable arrangement of the Cu active centers on a ZrO_x support (compare also Fig. 3(a) and (b)). This surface rearrangement certainly should include the coalescence of Cu crystallites, that is, an increase in particle size. This conclusion seems to be in agreement with specific surface area data indicating that after heat treatment, exposure to air and reaction, Cu(0) surface areas diminish (values smaller than 0.1 $m^2\,g^{-1}$ were measured).

Selectivities of the catalytic transformation of 2-propanol were also measured (Table 1). As seen, in addition to acetone the product of dehydrogenation, products of secondary reactions are also formed. It was already noted in our first paper disclosing the catalytic properties of amorphous Cu–Zr alloys, that methyl isobutyl ketone the product of a multistep transformation is always formed in various amounts [8]. The process starts with the dimerization of acetone to yield diacetone alcohol (DAA) (step 1) which readily undergoes elimination of water to form mesityl oxide (MO) (step 2). The carbon–carbon double bond of mesityl oxide is hydrogenated to yield methyl isobutyl ketone (MIBK) (step 3). Furthermore, the carbon–oxygen double bond of the latter product may also be hydrogenated to methyl isobutyl carbinol (MIBC) (step 4).

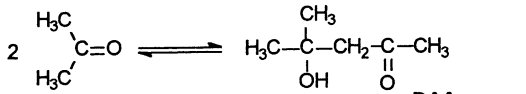

(1)

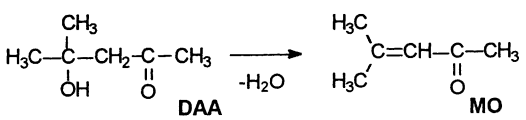

(2)

Table 1
Selectivities in the dehydrogenation of 2-propanol over a 1-year old amorphous 60Cu–40Zr alloy[a]

Sample	Acetone	MIBK[b]	MIBC[c]
As-received	89.9	6.7	3.4
Oxidized (473 K, 3 h)	90.1	8.1	1.8
Hydrogen-treated (393 K, $p_{H_2} = 0.12$ GPa, 70 h)	96.8	3.2	0
Hydrogen treatment followed by annealing (623 K, 5 h in He) and air exposure (2 days)	87.7	9.4	2.9
As above, but with longer air exposure (9 days)	86.6	9.4	4

[a] For reaction conditions, see Section 2.
[b] MIBK: methyl isobutyl ketone.
[c] MIBC: methyl isobutyl carbinol.

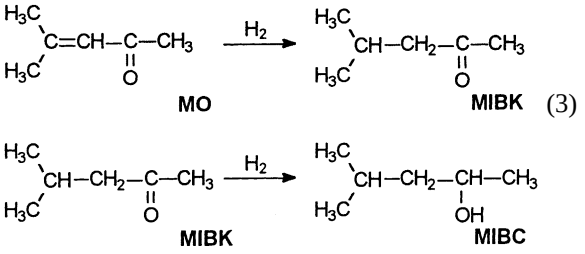

We showed in a detailed study [36] that formation of MIBK requires bifunctional catalysis. Dimerization of acetone is catalyzed by basic sites, in this case, by ZrO_2. Elimination of water is a facile process at the reaction temperature applied. Finally, copper is an active metal in both hydrogenation reactions. Selectivity data collected in Table 1 provides an important piece of information about the relative activity of the two catalytic functions of the various catalyst preparations. The high selectivity of acetone formation shows that copper is very active, whereas the number and strength of basic active sites of ZrO_2 are low. The high activity of copper is also manifested (i) by the fact that the intermediate MO is not detected and (ii) by the formation of the other by-product MIBC. Noteworthy is the lack of MIBC over the sample which underwent only the hydrogen treatment (Table 1, entry 2). This indicates, in general, the relatively low activity of metallic active sites of this sample just as in the main reaction, in the dehydrogenation of 2-propanol.

4. Summary and conclusions

Hydrogenation of Cu–Zr AA under high pressures and at temperatures up to 373 K results in an expansion of the inter-atomic distances in the bulk of the Cu–Zr amorphous alloys, brittleness of the bulk material, and formation of some surface microcracks where a partial Cu segregation and crystallization can start. This material exhibits low catalytic activity in the dehydrogenation of 2-propanol in spite of a large specific surface area developing in the catalytic reaction. However, after desorption of hydrogen at 623 K and subsequent air exposure at room temperature, the catalytic activity increases with exposure time. This points to the role of Zr oxidation to generate Cu active centers of suitable size and arrangement on a ZrO_x support for the catalytic process.

Acknowledgements

This work was financially supported by Grant KBN 7-T08C-046-19, by the Institute of Physical Chemistry, Polish Academy of Sciences, and by Grant FKFP 0377/1999 from the Ministry of Education of Hungary. Thanks are also due to M. Pisarek, M.Sc. for the preparation and examination of the cross-sections of the ribbons.

References

[1] K. Hashimoto, Mater. Sci. Eng. A226–A228 (1997) 891.
[2] Á. Molnár, G.V. Smith, M. Bartók, Adv. Catal. 36 (1989) 229.
[3] A. Baiker, Faraday Disc. Chem. Soc. 87 (1989) 239.
[4] H. Beck, H.-J. Güntherodt (Eds.), Glassy Metals III. Springer, Berlin, 1994, p. 122, 131.
[5] G. Ertl, H. Knözinger, J. Weitkamp (Eds.), Handbook of Heterogeneous Catalysis, VCH, Weinheim, 1997, Chapter 4.4, pp. 803–814.

[6] D. Stoychev, J. Ikonomov, K. Robinson, P. Stefanov, M. Stoycheva, T. Marinova, Surf. Interface Anal. 30 (2000) 69.
[7] H. Yamashita, M. Yoshikawa, T. Kaminade, T. Funabiki, S. Yoshida, J. Chem. Soc., Faraday Trans. 1 82 (1986) 707.
[8] Á. Molnár, T. Katona, M. Bartók, K. Varga, J. Mol. Catal. 64 (1991) 41.
[9] Á. Molnár, T. Katona, Cs. Kopasz, Z. Hegedüs, Stud. Surf. Sci. Catal. 75 (1993) 1759.
[10] T. Katona, Á. Molnár, J. Catal. 153 (1995) 333.
[11] A. Baiker, R. Schlögl, E. Armbruster, H.J. Güntherodt, J. Catal. 107 (1987) 221.
[12] C. Schild, A. Wokaun, A. Baiker, Fresenius J. Anal. Chem. 341 (1991) 395.
[13] C. Schild, A. Wokaun, A. Baiker, Surf. Sci. 269/270 (1992) 520.
[14] C. Schild, A. Wokaun, R.A. Koeppel, A. Baiker, J. Phys. Chem. 95 (1991) 6341.
[15] A. Baiker, D. Gasser, J. Lenzner, A. Reller, R. Schlögl, J. Catal. 126 (1990) 555.
[16] A. Baiker, M. Maciejewski, S. Tagliaferri, P. Hug, J. Catal. 151 (1995) 407.
[17] M. Janik-Czachor, A. Kudelski, M. Dolata, M. Varga, Á. Molnár, J. Bukowska, A. Szummer, Mater. Sci. Eng. A267 (1999) 227.
[18] A. Kudelski, M. Janik-Czachor, M. Varga, M. Dolata, J. Bukowska, Á. Molnár, A. Szummer, Appl. Catal. A 181 (1999) 123.
[19] M. Janik-Czachor, A. Szummer, Á. Molnár, M. Dolata, A. Kudelski, M. Varga, J. Bukowska, K. Sikorski, Electrochim. Acta 45 (2000) 3295.
[20] A. Baiker, H. Baris, H.J. Güntherodt, J. Chem. Soc., Chem. Commun. (1986) 930.
[21] A. Baiker, H. Baris, H.J. Güntherodt, Appl. Catal. 22 (1986) 389.
[22] T. Katona, Á. Molnár, V.I. Perczel, Cs. Kopasz, Z. Hegedus, Surf. Interface Anal. 19 (1992) 519.
[23] F. Vanini, St. Büchler, X.N. Yu, M. Erbudak, L. Schlappbach, A. Baiker, Surf. Sci. 189/190 (1987) 1117.
[24] A. Baiker, H. Baris, M. Erbudak, F. Vanini, in: L. Guczi, F. Solymosi, P. Tétényi (Eds.), New Frontiers in Catalysis, Elsevier, Amsterdam, 1993, p. 1928.
[25] F. Vanini, M. Erbudak, G. Kostorz, A. Baiker, Mater. Res. Soc. Symp. Proc. (Microstruct. Prep. Catal.) 111 (1988) 375.
[26] N. Ismail, M. Uhlemann, A. Gebert, J. Eckert, J. Alloys Compounds 298 (2000) 146.
[27] N. Ismail, A. Gebert, M. Uhlemann, J. Eckert, L. Schultz, J. Alloys Compounds 314 (2001) 170.
[28] B. Baranowski, S.M. Filipek, Synthesis of metal hydrides, in: J. Jurczak, B. Baranowski (Eds.), High-Pressure Chemical Synthesis, Elsevier, Amsterdam, 1989, pp. 55–100.
[29] K. Suzuki, J. Less Common Met. 89 (1983) 183.
[30] S.M. Filipek, A. Szummer, I. Marchuk, J. Alloys Compounds 293–295 (1999) 7.
[31] S.M. Filipek, A.B. Sawaoka, JHPI 30 (1992) 335.
[32] A. Szummer, M. Pisarek, M. Dolata, A. Molnar, M. Janik-Czachor, M. Varga, K. Sikorski, J. Metastable Nanocr. Mater., in press.
[33] R.J. Madix, Adv. Catal. 29 (1980) 1.
[34] M.A. Chester, E.M. McCash, Spectrochim. Acta 43A (1987) 1625.
[35] J. Cunningham, G.H. Al-Sayyed, J.A. Cronin, J.L.G. Fierro, C. Healy, W. Hirschwald, M. Ilyas, J.P. Tobin, J. Catal. 102 (1986) 160.
[36] V. Chikán, Á. Molnár, K. Balázsik, J. Catal. 184 (1999) 134.